Melanoma Dermoscopic Image Segmentation by Analyzing Color Features Using Active Contour Model

Rashmi Ashtagi[1*] , Sagar Mohite[2] , Mohammed Zakariah[3] , Abdulaziz S. Almazyad[4] , Deepak Mane[1] , Ranjeet Vasant Bidwe[5]

[1] Department of Computer Engineering, Vishwakarma Institute of Technology, Pune 411037, India
[2] Department of Computer Engineering, College of Engineering, Bharati Vidyapeeth Deemed University, Pune 411037, India
[3] Department of Computer Science and Engineering, College of Applied Studies and Community Services, King Saud University, Riyadh 11495, Saudi Arabia
[4] Department of Computer Engineering, College of Computer and Information Sciences, King Saud University, Riyadh 11543, Saudi Arabia
[5] Symbiosis Institute of Technology, Pune Campus, Symbiosis International (Deemed University) (SIU), Pune 412115, India

Corresponding Author Email: rashmiashtagi@gmail.com

ABSTRACT

Advanced diagnosis and successful treatment of melanoma depend on early detection, especially in light of the significant rise in melanoma cases in recent years. The suggested Active Contour Model (ACM) and machine learning (ML) techniques are used in this research to present a robust dermoscopic lesion image segmentation process for melanoma identification. By developing a strong association between forefront and background entities, the ACM effectively manages high-dimensional lesion image data, improving pixel detection performance and forming sharp edges and lesion pattern recognition. A Gaussian distribution model is used to control changes in pixel intensity. The comprehensive ISIC 2017 challenge dataset is used to assess the performance of the suggested ACM, and the PH2 dataset is used for extra validation. The testing outcomes demonstrate how well the suggested ACM segmented images in terms of segmentation accuracy, dice coefficient, and visual appeal. The abstract, however, may improve by addressing the clinical relevance of the suggested technique, outlining dataset sizes and potential biases, giving particular values for performance metrics selected, and delivering more information on the individual ML algorithms included in the ACM.

1. INTRODUCTION

1.1 Challenges and motivation

Long-term sun exposure that exposes oneself to damaging UV radiation is the main cause of melanoma. The likelihood of a satisfactory outcome from therapy is greatly increased when skin cancer is discovered early. However, a thorough grasp of numerous variables, including lesion shape, color, size, type, mutations, general look, and growth patterns, is necessary for an accurate diagnosis of melanoma. Skin specialists with extensive training, such as dermatologists, usually have this complex expertise. Even for experts, manually diagnosing skin cancer takes a lot of effort and time. Technology has been a big help to healthcare systems around the world, but one possible option is to use dermoscopic images to automatically diagnose skin cancer, especially melanoma. In order to prevail the difficulties, the ACM useful segmentation technique is suggested in this work. The work aspires to lead to a real-time detection of melanoma by closing the gap between expert knowledge and automated diagnosis using dermoscopic pictures with the application of an Active Contour Model.

Furthermore, the useful imaging modality is dermoscopy, which reduces reflections on the skin's surface [1]. Dermoscopy eases the diagnosis and viewing of skin lesions in the skin because it provides reduced reflections in the affected skin area [2]. Many studies confirm that dermoscopy performs better in diagnosis as compared to traditional photography [3], which is information a dermatologist should know when trying to diagnose skin cancer disorders. Whereas melanoma detection with the naked eye only from dermoscopic lesion images is challenging and erroneous, it may decrease the quality of life of skin cancer patients [4]. Therefore, to address this challenge, state-of-the-art technology like artificial intelligence, machine learning methods, or deep learning frameworks are necessary for implementation in order to realize an accurate diagnosis. In such a respect, incorporating these cutting-edge technologies into ACM would be an efficient method according to the context of the proposed research. This method specifically employs dermoscopic pictures to classify lesions with the goal of differentiating between melanoma and non-melanoma instances. Superior feature extraction and segmentation of

dermoscopic lesion images are critical to the success of such a classification procedure, and they are in accordance with the goals of the study described in the cited research.

In the study by López-Leyva et al. [5], an artificial neural network architecture is presented to detect skin cancer lesions based on the information from Fourier spectral images. This technique is implemented in the additive color model for multiclass diagnosis. Here, correlation coefficients are identified for effective lesion classification. Training and testing are conducted on varied datasets in order to achieve higher performance results in terms of precision, recall, and accuracy. In the study by Bian et al. [6], a filtered transfer learning method is adopted for skin lesion detection using labeled data. Here, the transfer learning method in the multi-view category determines significant discriminative information to generate weights for efficient lesion classification. In the study by Khan et al. [7], a lesion detection and classification technique are presented with the help of tele dermatology tool. This research article mainly focuses on the segmentation of lesion images and the classification of lesions through obtained features. Here, convolutional neural network architecture is also presented for saliency segmentation. In the study by Ain et al. [8], a melanoma identification technique is introduced based on obtained discriminative features. Here, the skin classification method is also presented to distinguish between melanoma and non-melanoma through obtained local information in color images. However, real-time implementation of these advanced technologies in traditional methods is quite challenging.

1.2 Objective and contribution

Thus, a highly suitable and proficient skin cancer detection technique is required to diagnose cancer diseases. Therefore, in this article, a melanoma detection technique is presented based on effective dermoscopic lesion image segmentation process to distinguish between melanoma and non-melanoma. Here, lesion segmentation is achieved using the proposed ACM through dermoscopic images based on ML techniques. Although classification of dermoscopic images is essential to differentiate between melanoma and non-melanoma lesions. However, segmentation is the first step in any image classification process, especially in the case of skin cancer diagnosis. Based on the effective segmentation results, high-quality gradient and discriminative contour features are generated, which helps in an efficient classification process. In this article, the proposed ACM provides sharp edges and smoother boundaries in lesion-segmented images with accurate shapes. Here, low-level and high-level contextual data are joined together to obtain quality segmented images from background and foreground entities of lesion images. Here, the proposed ACM forms a strong bond between pixels of foreground and background patches of lesion images. Experimental results demonstrate the superiority of the proposed ACM in terms of segmentation accuracy, dice coefficient, and visual appearance of segmented images.

• Creative Fusion of ML and ACM: The present study proposes the world's first fusion approach that integrates ACM's strength in lesion segmentation with the power of ML. This sort of integration aids in enhancing the accuracy and effectiveness of identifying early-stage melanoma.

• Enhanced Performance Assessment: The study conducts a thorough assessment of a wide range of machine learning (ML), deep learning (DL), and transfer learning (TL) architectures, going beyond traditional methods. This comprehensive analysis offers important benchmarking findings for the melanoma dermoscopic image segmentation issue in addition to information on the effectiveness of the suggested ACM.

• It has integrated several benchmark datasets; the paper contains the testing of known benchmark datasets, like PH2 and ISIC 2017, to be more generalizable and stronger on the proposed technique. In this way, this broader test gives evidence of the flexibility and versatility of the active contour model over many datasets.

• It also investigates and proposes optimized training procedures for applied ML, DL, and TL architectures in the study. This will provide a deep insight into learning approaches, model optimization, and parameter adjustment-very significant knowledge contributions toward further studies in this field.

This research is divided into the following sections; Section 1 provides the introduction to melanoma, Section 2 discusses the literature survey related to the detection of Melanoma skin cancer and their detection challenges, and how these challenges can be handled by researchers. Section 3 mentions the methodology and mathematical modelling utilized detection of Melanoma skin cancer using the proposed active contour model. Section 4 discusses dataset details, performance parameters, and experimental results and their comparison with state-of-the-art cancer identification techniques, and section 5 is the conclusion.

The body's largest and most important organ, the skin, acts as a barrier to protect the body from a variety of illnesses. But because the skin serves as the main barrier between the body and the outside world, it can become ill easily. Skin disorders can be difficult to diagnose since they frequently have similar signs and symptoms. The diagnosis of lesions related to skin cancer poses a significant challenge since it may result in DNA damage, which could allow aberrant cells to develop unchecked through various skin mutations. The need for efficient detection techniques is highlighted by the rise in the incidence of skin cancer worldwide, particularly melanoma. Classified as a malignant skin illness, melanoma is extremely dangerous, with an alarming fatality rate of 85% and a rapid global expansion. In order to meet the urgent need for sophisticated diagnostic methods, this research suggests an image segmentation strategy that makes use of the Active Contour Model. The suggested approach aims to support early and precise melanoma diagnosis by integrating the degree of melanoma with the requirement for complex image segmentation.

Besides, Melanoma is a type of malignant lesion which generated from melanocytes. Further, melanocytes are cells that contain pigments [9]. And rate of mortality is quite high in Melanoma in all cancer types. According to a report published by the American Cancer Society [10] in 2019, the United States of America (USA) encountered 96,480 fresh melanoma cases in the year 2019, and out of those, around 7,230 people are predicted to die due to melanoma disease. According to another American report, it is predicted that 9,500 people in the USA will be diagnosed with melanoma skin cancer every day, and one out of every five American people will have melanoma skin cancer in their lifetime [11]. In addition, various reports have claimed that there are 3 million American people affected with squamous cell carcinoma (SCC) and basal cell carcinoma (BCC) every year. Furthermore, the general BCC occurrence incidence in

America has enhanced by 145% from the period 1976-1984 to 2000-2010. In contrast, the rate of incidence is enhanced by 263% in the case of SCC, considering a similar time period [12]. Figure 1 shows the melanoma images from the ISIC 2017 dataset [13].
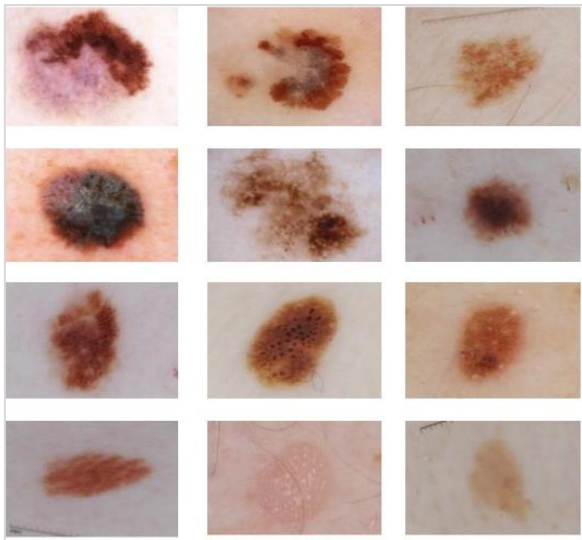

Figure 1. ISIC 2017 dataset images [5]

1.3 Challenges and motivation

Long-term sun exposure that exposes oneself to damaging UV radiation is the main cause of melanoma. The likelihood of a satisfactory outcome from therapy is greatly increased when skin cancer is discovered early. However, a thorough grasp of numerous variables, including lesion shape, color, size, type, mutations, general look, and growth patterns, is necessary for an accurate diagnosis of melanoma. Skin specialists with extensive training, such as dermatologists, usually have this complex expertise. Even for experts, manually diagnosing skin cancer takes a lot of effort and time. Technology has been a big help to healthcare systems around the world, but one possible option is to use dermoscopic images to automatically diagnose skin cancer, especially melanoma. Such challenges can be overcome with an important segmentation technique provided by the ACM proposed in this work. This work intends to fill up the gap between expert knowledge and automated diagnosis using Dermoscopic pictures and the Active Contour Model, probably making a breakthrough in real-time melanoma detection.

Dermoscopy remains a useful imaging modality that reduces reflections on the skin surface. Dermoscopy makes skin lesions easy to see, hence diagnosis, by reducing reflections in that particular part of the skin being considered for the lesion diagnosis. A number of studies further confirm that Dermoscopy performs better than traditional photography in terms of diagnosis. This was an important revelation that dermatologists are supposed to know at the time of diagnosis of disorders related to skin cancer. Detection of melanoma with the naked eye only from Dermoscopic lesion images is however challenging and erroneous. This affects the quality of life of skin cancer patients. Coupling state-of-the-art technology in artificial intelligence, machine learning methods, deep learning frameworks with ACM as deemed necessary for accurate diagnosis in the context of the proposed research. This method specifically employs dermoscopic pictures to classify lesions with the goal of differentiating between melanoma and non-melanoma instances. Superior feature extraction and segmentation of Dermoscopic lesion images are critical to the success of such a classification procedure, and they are in accordance with the goals of the study described in the cited research.

1.4 Objective and contribution

Thus, a highly suitable and proficient skin cancer detection technique is required to diagnose cancer diseases. Therefore, in this article, a melanoma detection technique is presented based on effective dermoscopic lesion image segmentation process to distinguish between melanoma and non-melanoma. Here, lesion segmentation is achieved using the proposed ACM through dermoscopic images based on ML techniques. Although classification of dermoscopic images is essential to differentiate between melanoma and non-melanoma lesions. However, segmentation is the first step in any image classification process, especially in the case of skin cancer diagnosis. Based on the effective segmentation results, high-quality gradient and discriminative contour features are generated, which helps in an efficient classification process. In this article, the proposed ACM provides sharp edges and smoother boundaries in lesion-segmented images with accurate shapes. Here, low-level and high-level contextual data are joined together to obtain quality segmented images from background and foreground entities of lesion images. Here, the proposed ACM forms a strong bond between pixels of foreground and background patches of lesion images. Experimental results demonstrate the superiority of the proposed ACM in terms of segmentation accuracy, dice coefficient, and visual appearance of segmented images.

• Creative Fusion of ML and ACM: The study presents a brand-new fusion strategy that combines the advantages of ACM lesion segmentation with the strength of ML techniques. This serves to enhance the accuracy and efficiency of early-stage melanoma identification.

• Improved Performance Evaluation: The present study goes on to present the detailed performance evaluation of a comprehensive portfolio of machine learning, deep learning, and transfer-learning-based architectures beyond some traditional approaches. This thorough analysis presents some key benchmarking results for the melanoma dermoscopic image segmentation problem, apart from details about the efficiency of the proposed ACM.

• Evaluation of several well-known benchmark datasets: In the paper, some of the well-known benchmark datasets, like PH2 and ISIC 2017, have been evaluated to establish the generality and strength of the proposed technique. This extended test bench speaks to the flexibility and adaptability of the Active Contour Model across many such datasets.

• Optimized training procedures: The study investigates and proposes optimized training procedures for the ML, DL, and TL-based architectures used in this study. It informed insight into learning approaches to model optimization and parameter adjustments-relevant knowledge contributions for the next studies in this field.

This research is divided into the following sections; Section 1 provides the introduction to melanoma, Section 2 discusses the literature survey related to the detection of Melanoma skin cancer and their detection challenges, and how these challenges can be handled by researchers. Section 3 mentions the methodology and mathematical modelling utilized

detection of Melanoma skin cancer using the proposed active contour model. Section 4 discusses dataset details, performance parameters, and experimental results and their comparison with state-of-the-art cancer identification techniques, and section 5 is the conclusion.

2. LITERATURE SURVEY

Recently, skin cancer cases have increased drastically due to ever-increasing global warming. Thus, melanoma detection in earlier stages is of great importance. Furthermore, the lowest survival rate of melanoma patients is a concerning area and makes melanoma one of the deadliest cancer diseases worldwide. Thus, several researchers have recommended that a detailed study of skin lesion images can be of great importance in handling skin cancer diseases. Nevertheless, *Dermoscopic* lesion image study is heavily impacted by three major steps such as lesion segmentation, feature extraction, and lesion classification. Thus, the first step to analyse *Dermoscopic* image lesions are the segmentation of lesion images to diagnose skin cancer. Therefore, numerous researchers have carried out immense work in this domain for Melanoma disease analysis. Some of the current research articles have been discussed in the following paragraph.

2.1 Machine learning techniques

Rehman et al. [14] developed a method centered on locating and removing hairs or edge borders from dermoscopy pictures. This was done in order to improve the image and remove lesions using the machine learning-based GrabCut method. On the PH2 and ISIC2018 datasets, respectively, the assessment findings showed Jaccard Index values of 0.77 and 0.80 coupled with Dice index values of 0.87 and 0.82. The assessment, however, does not go into great detail about the limitations and implications of various metrics, like the Dice coefficient and the Jaccard Index. Readers would benefit from more detailed information regarding why certain indicators were chosen and the interpretation of their nuanced meaning to firmly establish the effectiveness of the suggested segmentation strategy.

In the study by Seeja and Suresh [15], color, texture, and shape features are extracted from segmented images using various techniques such as Local Binary Pattern, Histogram of Oriented Gradients, Edge Histogram, and Gabor techniques. Segmentation is done through the U-net algorithm, which is a Convolutional Neural Network. Extracted features are used in classifying skin images into benign lesions or melanoma by being fed into classifiers like Random Forest, K-Nearest Neighbor, Support Vector Machine, and Naive Bayes. Results in these studies were very encouraging, with accuracy of 85.19 percent for the SVM classifier and a Dice coefficient value of 77.5 percent for image segmentation.

2.2 Deep learning techniques (DL)

In previous study [16], an automated lesion segmentation method is presented for the identification of melanoma skin cancer detection based on a mutual bootstrapping model. Here, the authors use deep CNN architecture for efficient conduction of the lesion classification process. In the study by Berkay et al. [17], an automatic skin cancer detection technique is introduced based on the DL model and reduces limitations faced in melanoma detection. Here, effective feature maps are generated for effective pixel-wise image classification using encoder and decoder mechanisms. In the study by Putra et al. [18], a dynamic augmentation process is utilized for skin cancer estimation based on machine learning techniques. Here, effective and dynamic training and testing is conducted for efficiency enhancement. In addition, the Bayesian optimization method is adopted to speed up the training process. In the study by Zhao et al. [19], generative adversarial networks (GANs) architecture is presented for skin lesion augmentation, which improves the efficiency of Dermoscopy Image Classification. This model enhances the accuracy of the lesion classification process. In addition, DenseNet201 architecture is presented to reduce noise and reconstruct images. Their experimental results show that the classification framework performs well on the ISIC2019 dataset, and the BMA reaches 93.64%. In the study by Pacheco and Krohling [20], an attention-based mechanism is presented to perform classification on skin lesion images using deep learning models. Here, an attention-based mechanism joins image, and metadata image information for skin cancer classification. The Metadata Processing Block method is utilized for metadata feature extraction. In the study by Rastghalam et al. [21], a Hidden Markov Model (HMM) based asymmetric analyser is adopted for skin cancer identification in earlier stages. Here, an asymmetric analyzer is utilized to obtain texture heterogeneity. Statistical histogram features are generated to ensure efficient melanoma detection. In previous studies [22, 23], the ensemble of multi-layer perceptron and CNN is used.

2.3 Transfer learning techniques (TL)

A residual Neural Network Architecture for skin cancer detection and classification is presented by Razzak and Naz [24]. The presence of a residual network with a transition layer in this architecture makes feature representation efficient. The residual learning mechanism is utilized for the efficient classification of skin cancer diseases. In the study by Adegun and Viriri [25], a detailed survey is presented on varied skin cancer detection techniques based on DL and ML methods. Here, several challenges and issues faced by numerous researchers are discussed, and to mitigate them, different solutions are suggested. Patil and Bellary [26] use the TL method. The model they proposed used a pre-trained Transfer Learning model. They were able to separate three types of melanoma: lentigo maligna melanoma, nodular melanoma, and superficial spreading melanoma. Also, it is clinically important to know exactly where the uneven edges of melanoma skin lesions are. Choosing the exact lesion border is one of the hardest things to do. To solve the problem, they used a different method to find the edge of a cancerous area.

The introduction of automated systems for the detection of skin cancers may bring about definite improvements in patient outcomes. Skin cancer, if detected in its earliest stages, can be potentially treatable. Automated diagnostic systems can correctly and instantly analyze a case to detect it early enough. Such early detection might mean better survival rates and, later, a decrease in aggressive treatment modalities that are common in advanced-stage cancers. The proper delineation of the skin lesion boundaries is essential for lesion malignancy discrimination; therefore, segmentation should be pretty precise. A precise segmentation allows an appropriate evaluation of a dermatological lesion's characteristics, such as shape, size, and border irregularity, which are critical factors

in skin cancer diagnosis. There is also the role of automated detection devices in improving current treatment strategies through accurate and consistent evaluation of skin lesions, thus aiding clinicians to make more informed decisions about biopsy, treatment plans, and follow-up care. The integration of these systems into clinical practice improves diagnostic accuracy by reducing the chances of misdiagnosis and unnecessary procedures.

The above-discussed research works present varied methods for effective Melanoma segmentation processes through *Dermoscopic* images. However, real-time implementation of these methods has multiple problems, especially in the case of *Dermoscopic* image segmentation. Those problems are the presence of irregularities in feature identification, color symmetry problems, varied lesion sizes and their positions, and the presence of intrinsic characteristics like hairs, reflections, etc. Thus, an effective lesion segmentation method is introduced based on the ACM for Melanoma identification in the initial stages, and solutions for Melanoma segmentation problems are also discussed.

3. MODELS AND ALGORITHMS

The suggested melanoma detection system design follows a step-by-step procedure starting with dataset pre-processing and ending with the segmented picture output. The pre-processing stage starts with the Melanoma dataset and involves necessary actions like pixel detection and scaling. The next step is featuring extraction, which creates a connection between lesion structures to enable efficient identification. Gaussian distribution modeling is used in the segmentation procedure to differentiate between melanoma, atypical, and normal lesions. Lesions are divided into several classes using multi-class categorization. For lesion segmentation over several patches, the ACM is used; unary potentials and paired potentials are used for more accurate findings. Resulting in a segmented image, improving diagnosis precision and helping the dermoscopic images to identify melanoma effectively. Figure 2 shows the proposed system architecture.

3.1 Methodology

Basically, dermoscopic lesion segmentation is data processing where the steps initiate with the selection and pre-processing of the dataset. This would involve image enhancement using CLAHE and removal of blurring using the

Wiener filter technique. Detection of pixels in the foreground and background portions is carried out subsequently. This is followed by feature extraction. The next step is segmentation based on the Gaussian distribution model, which essentially involves separating the affected skin lesion as accurately as possible. The model also estimates probabilities for multi-class problems and uses unary and pairwise potentials for lesion segmentation. Advanced machine learning methods, such as FCN AlexNet, FCN-32s, FCN-16s, FCN-8s [27], DeepLab V3+, Mask R-CNN [28], and Ensemble-L, are employed for classification. Finally, an Active Contour Model (ACM) handles multiple patches in dermoscopic lesion images, ensuring accurate segmentation. This study outlines the approach as a series of broad but interconnected phases.

Data Processing
1) Dataset Selection
2) Data Pre-processing
(a) Image Enhancement Using CLAHE (Contrast Limited Adaptive Histogram Equalization)
(b) Wiener Filter is used to reduce blurring in images.
3) Pixel detection performance calculation of background and foreground image

Feature Extraction
4) Relationship established between forefront and background image entities
5) Lesion structures extraction from the background
6) Segmentation using the Gaussian distribution model

Modelling
7) Probability Estimation Calculation for Multi-class Problem
8) Modelling of Lesion Segmentation Process using Unary Potentials
9) Modelling of Lesion Segmentation Process using Pairwise Potentials

Classification
10) Machine Learning Based Classification using FCN AlexNet, FCN-32s, FCN-16s, FCN-8s, Deeplab V3+, Mask R-CNN, Ensemble-L
11) ACM for Multiple Patches in Dermoscopic Lesion Images

The following subsection provides an in-depth description of the steps involved in the melanoma dermoscopic image segmentation process.
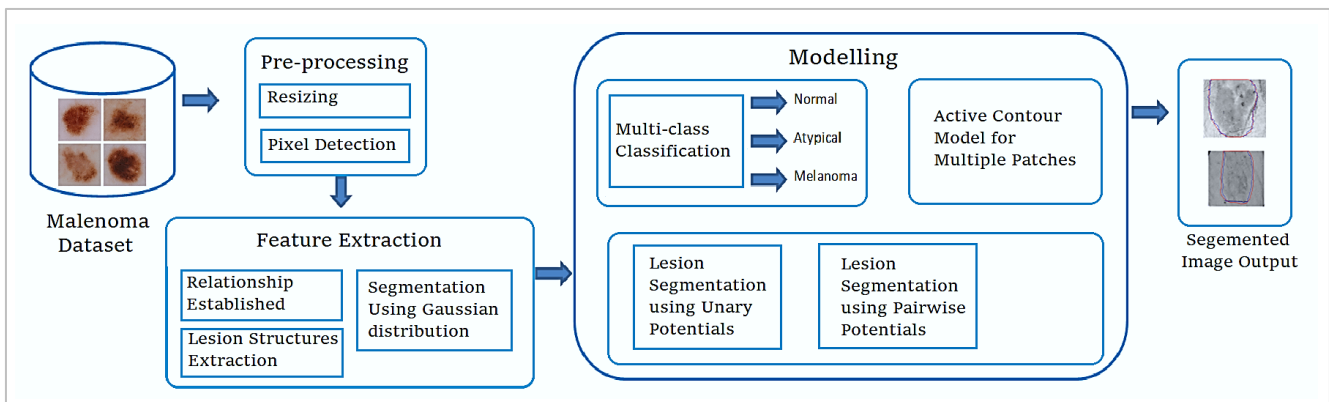

Figure 2. Proposed system architecture

3.2 Lesion segmentation using active contour model

In this section, a detailed mathematical modeling of the proposed ACM is presented to perform an efficient lesion segmentation process for effective diagnosis of Melanoma skin cancer disease. Moreover, high dimensional lesion image data can be efficiently handled using the proposed ACM. Here, pixel detection performance is mainly improved based on the strong relationship established between forefront and background image entities to form sharp edges and recognize patterns of lesion images in the segmentation process. Here, low-level and high-level image information are utilized together to extract lesion structures from the background. Furthermore, a detailed modeling for the lesion segmentation process is given in the following section.

The Neural Network Modelling components are offered by the DLS, a Model Driven Architecture Tool, in the form of a stack of drag-and-drop and create art. The following is an outline of the significant basic stages that were engaged in the research technique used in this research:

It is evident from several kinds of literature that the classification of lesion images is highly significant in distinguishing between melanoma and non-melanoma lesion images. Thus, the classification process consists of three crucial phases; which first is the efficient segmentation of *dermoscopic* lesion images, the second is a high-quality feature extraction process, and the final phase is a classification of obtained features to differentiate between melanoma and non-melanoma lesion images. Therefore, skin cancer lesion image segmentation is a classification problem and is modeled using multiple labels. Moreover, dermoscopic lesion images are split into multiple patches, and these patches are marked against different labels. Here, Gaussian distribution model $T=(K, S)$ is utilized to form properly segmented structures with sharp lesion edges S and lesion vertices K where all patches of lesion images belong to one of the particular class R. For a given image, consider that u is a vector which represents lesion data with dimensions $Z \times Z$. Here, the elements of data vector u is formed using observed variables as $(u_1, u_2, u_3, \ldots, u_\sigma)$. Here, number of patches are denoted as σ. Then, in case of multi-color bands, the colored pixel value is denoted as u at specified wavelength a. Then, m is defined as their corresponding segmented label which belongs to R^Q and here, R represents the number of classes. Moreover, all the edges remain in direct contact with image pixels, which helps in the mapping of contour features. Gaussian distributed model requires a bias region to model contour features, and a bias region is defined as a pixel set in which pixels can communicate with each other. Then:

$$y(m) = P^{-1} exp\left(-\sum_R \theta_R(u_R)\right) \qquad (1)$$

where, P denotes a constant coefficient and R shows bias region. And probability density function θ is utilized to normalize pixel values and mapping of feature vectors. Thus, bias region is modelled as:

$$y(m \backslash \{m_b\}) = y(\gamma(m_b)) \qquad (2)$$

where, $\gamma(m_b)$ is expressed as the group of pixels which belongs to another class as m_b. Here, the term $m \backslash \{m_b\}$ shows that pixel m_b is excluded from all the image pixels, and generated contours can be denoted as (U, M). Then, feature space

corresponding to active contour U is expressed by following equation:

$$Y(u) = P^{-1} exp\left(-\left[\sum_{\varphi \in K} \beta S_j(m_\varphi, U)\right] + \sum_{<b,i> \epsilon S} \chi S_y(m_b, m_i, U)\right) \qquad (3)$$

where, β and χ represent obtained feature weights. Moreover, unary and pairwise potentials are represented by variables S_j and S_y respectively. Strong communication is being set up between contour features and lesion labels using unary potential S_j whereas pairwise potential S_y is utilized to control numerous illustrations related to adjacent pixels. Here, all the adjacent pixels are assigned a similar label. Further, both unary and pairwise potential are functions of obtained contour features U. Besides, pairwise potential S_y obtained at every edge is the function of all contour values as well as labels. And coefficient P is utilized as a normalizing parameter. In the proposed ACM, three major factors required to model a probability density function in the segmentation process are as follows. The first aspect discusses setting up a strong relationship between input images and labels. Further, the second aspect discusses lesion edges that must communicate with all image patches and should follow spatial restraints. The final aspect is about label constraints in neighboring color bands. Strong modeling of these aspects provides an efficient and stable lesion segmentation with accurate structures. A combined energy of unary potential S_j, pairwise potential S_y and color band energy S_e makes an energy model for contours. Then, color image embedding is determined using the ACM.

3.3 Modelling of probability estimation for multi-class problem

In this section, comprehensive mathematical modeling for probability estimation for object class selection is presented to handle the multi-class problem that occurs in a lesion segmentation process. Consider an unknown pixel b, the class label is expressed as m_b in the lesion segmentation evaluation process. In a multi-class problem, for a class label m_b, the probability of object class selection is given by following equation:

$$m_b = \arg y(u) \qquad (4)$$

where, observed image features are expressed by u, and different feature weights are generated using ACM to get efficient lesion segmentation. Generated contour feature weights can be utilized in Eq. (4). In addition, $y(u)$ estimation is performed based on low-level contextual information. Much literature finds it difficult to determine the probability of $y(u)$ in the lesion segmentation process using low-level contextual information. Thus, in the case of high-intensity variations in pixels, model accuracy decreased in those models. Therefore, solutions to handle high-intensity variations are discussed in this article using the proposed ACM. This can be achieved by reducing the unnoticeable feature space of particular classes. The proposed ACM maps all the image pixels in each observation, considering unobserved class variables $p_q \in p_1, \ldots \ldots, p_Q$. Here, input image data is represented by an observation matrix, which is made up of rows f and columns c. Thus, histogram gradients are evaluated considering each image patch. Then, the column probability considered is $Y(c_b)$ whereas the class probability considered is $Y(c_b)$, then row probability can be considered as $Y(p_q)$. Then, the final

combined probability is represented by the below equation:

$$Y(c_b, f_i) = \sum_{q=1}^{Q} Y(p_q)Y(C_b)Y(f_i) \quad (5)$$

where, Eq. (5) can be rewritten as:

$$Y(c_b, f_i) = Y(c_b).Y(p_q).\left(\sum_{j}^{Q} Y(p_j).y(c_b)\right)^{-1} \quad (6)$$

Here, high-quality segmentation is achieved by substituting a class label m in place of image information p, and obtained features are represented by color histogram gradients. All the obtained histogram gradients from each pixel, considering multiple color bands, are summed up to get the final color histogram. Then, feature weights are generated from the obtained final color histogram. These generated feature weights are capable of handling intensity variations in the lesion segmentation process using an ACM.

3.4 Modelling of lesion segmentation process using unary potentials

This section discusses the mathematical modeling of the lesion segmentation process using Unary potentials in the ACM. Here, Unary potentials work as a measuring coefficient to evaluate the probability of pixel b which will take class label m_b. Here, the Probability Density Function (PDF) is employed to remodel unary potential S_j in Eq. (3). PDF is utilized for mapping feature weights obtained from the varied observations of color histogram gradients corresponding to a class label q. Whereas intensity variations in pixels of an image are controlled using the Gaussian distribution function considering multiple color bands. Let a class that represents multiple color bands be defined by R. Then, the color histogram density function q_s at pixel b can be evaluated as:

$$y_r(u_b) = exp\left(-\frac{1}{2}(u_b - h_q)^I \Sigma^{-1}(u_b - h_q)\right).\left((2\pi)^{\frac{R}{2}}|\Sigma|^{\frac{1}{2}}\right)^{-1} \quad (7)$$

where, $h_q \in D^R$, $u_b \in D^R$ and $\Sigma \in D^{R \times R}$.

Finally, the probability of pixel b with respect to class label q considering unary potential is evaluated as:

$$S_j(u) = \beta^I. - \log\big(y(c, f_b)\, y_r(u_b)\big) \quad (8)$$

For a color image, observation value with respect to pixel b is represented by u_b and β represents weights, which are utilized for mapping bias regions and pixels.

3.5 Modelling of lesion segmentation process using pairwise potentials

This section discusses the mathematical modeling of the proposed lesion segmentation process using pairwise potentials, which works as a measuring coefficient to evaluate the frequency of communication by class labels placed at neighboring boundaries to the pixels of the image. Here, two pixels b and i are utilized in pixel and class label communication considering pairwise potentials. Let that same label be used for all the pixels located in the neighboring area. Then:

$$S_y(u) = 1 - \aleph(m_b, m_i) \quad (9)$$

where, the delta function is expressed by a variable $\aleph$ and the noise present in the class label can be reduced using the proposed contour model, which can work as a low-pass filter. Besides, image gradients are used to generate weight coefficients with respect to pairwise potentials. Then, pairwise potential in the spatial domain is evaluated as:

$$S_y(u) = \begin{cases} 0 & if\ m_b = m_i \\ \chi e^{-\lambda_b} & if\ m_b \neq m_i \end{cases} \quad (10)$$

where, χ is defined as the weight coefficient and pixel gradients are expressed by λ_b. RGB color domains in a color image, λ shows max rate of change. Evaluate vectors K_1 and K_2 at an angle Θ in u and m domain considering pixel b:

$$K_1 = \frac{dR}{du}r + \frac{dG}{du}g + \frac{dB}{du}b \quad (11)$$

$$K_2 = \frac{dR}{dm}r + \frac{dG}{dm}g + \frac{dB}{dm}b \quad (12)$$

where, red, blue and green color components are defined by R, G and B respectively in rgb domain. Then, gradient vector normalization $L(\Theta)$ considering pixel b using L_2 norm can be evaluated by following equation:

$$L\Theta = y\Theta + v\Theta + 2.isin^2\Theta\ cos^2\Theta \quad (13)$$

where, $i = K_1 \times K_2$ and $y = |K_1|^2, v = |K_2|^2$ and gradient vector $L(\Theta)$ becomes maximum at an angle Θ_0.

$$\Theta_0 = 0.5 \arctan(2i.(y - v)^{-1}) \pm \frac{\pi}{2} \quad (14)$$

where, color image gradients λ_b is determined as $\lambda_b = L(\Theta_0)$.

3.6 Active contour model for multiple patches in Dermoscopic lesion images

This section discusses the implementation of a multi-patches enabled ACM, considering *Dermoscopic* lesion images. The traditional lesion segmentation method contains only unary and pairwise potentials to distinguish between melanoma and non-melanoma lesion images. However, in the proposed Active Contour Model, labels selected for every pixel region are affected by the labels of neighboring pixel regions along with local influencing factors. Broadcasting of label information inside those regions depends upon the pixel connectivity in that region. Thus, consider an image pixel b in a i-th patch whose labels are connected to the neighboring pixels $m_{b',a_i'}$. Here, the adjacent wavelength is expressed by a_i' and b' corresponds to pixel b in 2-D space. Then, broadcasting of label information in an image for ACM using Bayes' Rule is given by the following equation:

$$y(u) = y\left(m_{b',a_i'}, u\right) * y(u) \quad (15)$$

where, considering that labels are placed at varied wavelengths which are conditionally independent of the observed neighboring pixel data, then Eq. (16) can be rewritten as:

$$y(u) \propto y\left(m_{b',a_i'}, u_{a_i}\right) \quad (16)$$

where, for every color image B_{a_i} with observations u_{a_i}, consider conditionally independent relationship between

labels and observed neighboring pixel data is established and wavelength is represented by a_i. Then, local mapping can be established by predicting mean and variance of pixel intensity variations using the Gaussian distribution model $y_a(u_{a_i})$. Then, the unary potential for the lesion segmentation process demonstrated in Eq. (17) can be changed accordingly:

$$S_j(u) = \beta^I. -log\left(y(c, f_b)\, y_a(u_{a_1,b})\, y_a(u_{a_i,b})\dots y_a(u_{a_{\sqsupset},b})\right) \qquad (17)$$

where, the number of color images in the frequency domain is represented by $\sqsupset$ and observation value with respect to pixel b in a color image is given by $u_{a_i,b}$ at wavelength a_i and weight coefficient vectors generated from color images are used to balance the mapping of pixels in bias regions and local entities. Here, this novel active contour model not only depends upon unary and pairwise potentials but is also affected by the labels of respective pixels present in the adjacent wavelength region. The presence of potentials inspires continuous labeling in adjacent wavelength regions. Here, color image gradients are determined by the average intensity variation evaluation for every pixel and their neighbors. Consider that continuous labeling in adjacent wavelength regions with respect to the pixel b is represented by a function $f_b(a)$, then image gradients $r(\lambda_{ba_i})$ in frequency domain with respect to pixel b at wavelength a_i is expressed as $\frac{df_b}{da}|_{a=a_i}$. Then, modelling of potentials in the frequency domain can be determined in reference to pairwise potential determined in spatial domain from Eq. (10):

$$S_e(u) = \begin{cases} 0 \ \ \text{if } m_{b,a_i} = m_{b',a_i'} \\ \Psi\ \dfrac{1}{r(\lambda_{ba_i})}\ \text{if } m_{b,a_i} \neq m_{b',a_i'} \end{cases} \qquad (18)$$

where, Ψ is defined as a weighting coefficient. Lastly, join all unary, pairwise potential and gradient potential measurements in frequency domain considering multiple patches together to determine energy function of ACM as:

$$S(u,\Theta) = S_j(u) + \sum_{i \in \gamma(b)} S_y(u) + \sum_{i \in \sqsupset} \sum_{b' \in \{\gamma(b),b\}} \sum_{a_i' \in \gamma(a_i)} S_e(u) \qquad (19)$$

where, adjacent pixel regions are represented by γ and weighting coefficients for unary, pairwise, and gradient potential in the frequency domain are expressed by $\Theta = \{\beta, \chi, \Psi\}$ and achieved in the training of images using ACM. Then, probability distribution considering labels is given by:

$$y(u) = P^{-1} e^{-\sum_b S(u)} \qquad (20)$$

where, P is defined as a normalizing parameter and expressed by the following equation:

$$P = \sum_m e^{-\sum_b S(u)} \qquad (21)$$

3.7 Optimal solution for energy function minimization

This section discusses the optimal solution to minimize energy in the proposed active contour model. Then, for a given training sample set $\{u^n, m^n\}$ where number of training samples

is given by N and ($n=1, 2, 3, \dots, N$). Here, energy is minimized by eliminating loss function in the training set for accurate labeling of test images. Then, the energy function of Eq. (19) can be rewritten with respect to Θ as:

$$S(u,\Theta) = \Theta^I \theta(u, m) \qquad (22)$$

where, a set of unary, pairwise, and gradient potentials in frequency domain are expressed by θ. Then, energy minimization is achieved by following the equation:

$$2^{-1}\|\Theta\|^2 + \sum_{n}^{N} \varrho_n \qquad (23)$$
$$s.t\ S(u^n, \Theta) - S(u^n, \Theta) \geq \lambda(m, m^n) - \varrho_n, \forall_n, \forall_m$$

where, the given label for *n-th* training sample is expressed by m^n and loss function is defined by evaluating cost between ground truths m^n and segmented result m as $\lambda(m, m_n)$. Then, loss function for multi-class problem is given by: $\lambda(m, m_n) = \begin{cases} 1, \text{if } m \neq m_n \\ 0, \text{otherwise} \end{cases}$.

Then, energy minimization function is given by, $f(\Theta)$ is represented as an objective function.

$$f(\Theta) = 1/2\|\Theta\|^2 + \sum S(u_n, \Theta) + (\lambda(m, m_n) - S(u_n, \Theta)) \qquad (24)$$

4. RESULTS AND DISCUSSION

In this section, the performance of the segmentation process using the Active Contour Model, details of PH2 and ISIC Challenge 2017 Dataset, ground truth preparation, and details of performance metrics are discussed. In this article, the proposed active contour model provides mathematical modelling for an effective segmentation process using unary potential, pairwise potential, and image gradient potential in the frequency domain, and a solution to minimize total energy is also discussed. Here, artifacts are eliminated with the help of the Gaussian distribution model and filters to get efficient contour features. Proper detection of lesion edges improves segmentation efficiency.

4.1 Dataset details

PH2 Dataset: The performance of the proposed active contour model is tested on PH2 Dermoscopic lesion images [13]. This dataset contains a total number of 200 dermoscopic lesion images. Out of 200 lesion images, 160 images are naevus type which further segregated into atypical naevus and common naevus category. Each category consists of 80 images. Rest images come under the Melanoma category. In this dataset, lesion images generate accurate and sharp edges. This dataset is utilized to validate the performance of the proposed active contour model on different datasets. Table 1 shows detailed dataset description.

ISIC-2017 lesion Segmentation Dataset: The International Skin Imaging Collaboration (ISIC) Dataset is one of the best-equipped lesion image datasets to test skin segmentation performance [28]. ISIC-2017 lesion Segmentation Dataset is a digital dataset that is formed through expert observations from across the world. This dataset is formed to provide automated solutions in the segmentation of skin lesion images and differentiate

efficiently between melanoma and non-melanoma. This community conducts skin lesion challenges every year to influence researchers from worldwide and enhance the diagnosis efficiency skin lesion detection process. This community also works on spreading knowledge regarding skin cancer disease and the use of *dermoscopic* lesion images. This dataset consists of a total number of 2750 images in which all images are segregated into three sets named as training set, testing set, and validation set. Here, the first set contains 2000 images, the second set consists of 600 images, and the third set contains 150 images. The proposed active contour model is trained upon a training set, and performance results are evaluated using the training set. The training set images are segregated into three categories 1372 normal nevus images, 374 Melanoma images and 254 keratosis images. Table 2 shows a detailed dataset description.

Table 1. PH2 dataset description

Type	Number of Images
Melanoma	40
Benign	160
Total	200

Table 2. ISIC 2017 dataset description

	Melanoma	Keratosis	Benign	Total
Training Dataset	374	254	1372	2000
Testing Dataset	117	90	393	600
Validation Dataset	30	42	78	150
Total	521	386	1843	2750

4.2 Performance parameters

The following are the metrics used for evaluation: specificity, sensitivity, accuracy, dice, and Jaccard index.

$$Sensitivity = \frac{\overrightarrow{TP}}{\overrightarrow{TP} + \overrightarrow{FN}}$$

$$Specificity = \frac{\overrightarrow{TN}}{\overrightarrow{TN} + \overrightarrow{TP}}$$

$$Accuracy = \frac{\overrightarrow{TP} + \overrightarrow{TN}}{\overrightarrow{TP} + \overrightarrow{TN} + \overrightarrow{FP} + \overrightarrow{FN}}$$

$$DI = \frac{2 * |\overrightarrow{A} \cap \overrightarrow{B}|}{|\overrightarrow{A}| + |\overrightarrow{B}|}$$

$$JA = \frac{|\overrightarrow{A} \cap \overrightarrow{B}|}{|\overrightarrow{A} \cup \overrightarrow{B}|}$$

where, $\overrightarrow{TP}$ =True Positive; $\overrightarrow{TN}$ =True Negative; $\overrightarrow{FP}$ =False Positive; $\overrightarrow{FN}$ =False Negative.

4.3 Experimental setup

The proposed active contour model is implemented on 64-bit Windows 10 OS and 16 *GigaBytes* (GB) RAM with Intel processor to get proper and efficient segmentation results. The performance of the proposed active contour model is evaluated considering performance metrics like Dice coefficient (DI), segmentation accuracy (AC), and *Jaccard* index (JA).

4.4 Result comparison

This section describes the performance comparison of segmented lesion images against several state-of-art segmentation techniques considering performance metrics like Dice coefficient (DI), segmentation accuracy (AC), and *Jaccard* index (JA). The efficiency of the proposed active contour model is validated using the PH2 and ISIC challenge 2017 dataset.

Here, Table 3 demonstrates quantitative performance considering PH2 dataset. All the performance metrics show great improvement in segmentation quality against recent state-of-art-segmentation methods such as FCN-16s [29], Deeplab V3+ [30], mask–RCNN [30], Ensemble-S, Ensemble-L, Ensemble-A [31]. Here, the performance parameters considered are Accuracy (AC), *Jaccard Index* (JA) Sensitivity, Specificity, and Dice Coefficient (DI). Here, the performance of the proposed active contour model provides a segmentation accuracy result of 96.77, a Jaccard index of 88.95, a Dice coefficient of 93.97, a specificity of 97.59, and a sensitivity of 98.98. It is validated from the performance results of Table 1 that the proposed contour model performs superior to several presented traditional segmentation techniques considering the PH2 dataset. Figure 3 shows the Qualitative Performance Analysis of the Proposed Active Contour Model against different Segmentation techniques on the PH2 dataset.

Table 3. Performance evaluation metrics (%) for lesion segmentation considering PH2 dataset

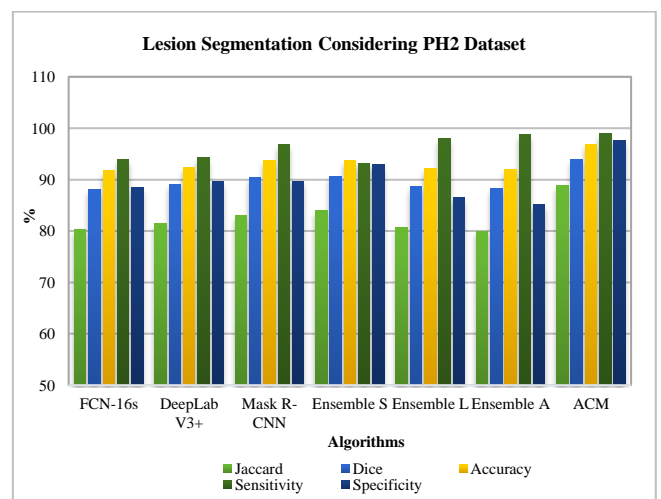| Algorithm	Jaccard	Dice	Accuracy	Sensitivity	Specificity
FCN-16s	80.20	88.10	91.70	93.90	88.40
DeepLab V3+	81.40	89.00	92.30	94.30	89.60
Mask R-CNN	83.00	90.40	93.70	96.90	89.70
Ensemble S	83.90	90.70	93.80	93.20	92.90
Ensemble L	80.60	88.70	92.20	98.00	86.50
Ensemble A	80.00	88.30	91.90	98.70	85.10
ACM	88.95	93.97	96.77	98.98	97.59

Figure 3. Qualitative performance analysis of proposed active contour model against different segmentation techniques on PH2 dataset

Similarly, Table 4 demonstrates quantitative performance considering the ISIC-2017 challenge dataset. All the performance metrics show great improvement in segmentation quality against recent state-of-art-segmentation methods such as the CDNN model [31], U-net1, U-net2 [32], Seg Net [33], FrCN, Ensemble-S, Ensemble-L, Ensemble-A. Here, the performance parameters considered are Accuracy (AC), *Jaccard Index* (JA), Specificity and Dice Coefficient (DI). Here, the performance of the proposed active contour model provides a segmentation accuracy of 94.63, a Jaccard index of 79.23, a Dice coefficient of 87.26, and a specificity of 98.58. It is validated from the performance results of Table 2 that the proposed contour model performs superior to several presented traditional segmentation techniques considering ISIC-2017 challenge dataset. Figure 4 shows the Qualitative Performance Analysis of the Proposed Active Contour Model against different Segmentation techniques on the ISIC 217 dataset.
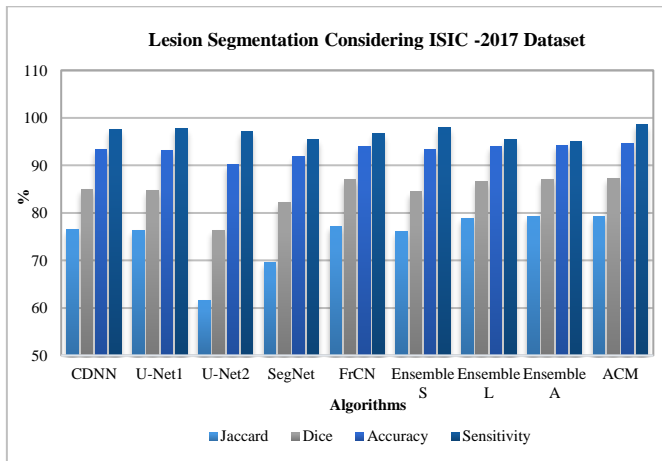

Figure 4. Qualitative performance analysis of proposed active contour model against different segmentation techniques on ISIC 217 dataset
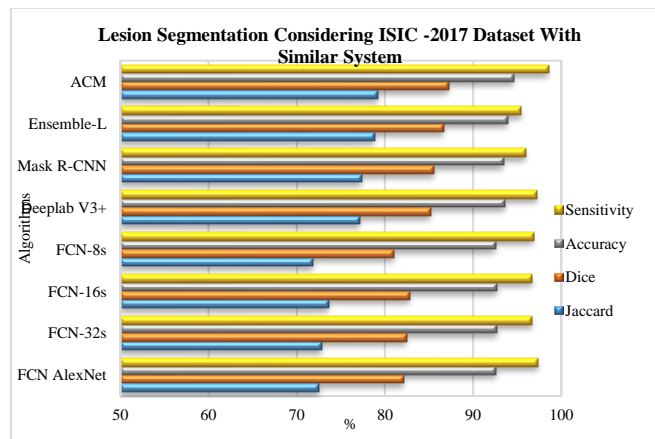

Figure 5. Qualitative performance analysis of proposed active contour model against different segmentation techniques

Similarly, Table 5 demonstrates quantitative performance considering ISIC-2017 challenge dataset against recent state-of-art-segmentation methods such as FCN AlexNet [34], FCN-32s, FCN-16s, FCN-8s, Deeplab V3+, Mask R-CNN, Ensemble-L [27]. Here, Table 5 performs superior to several presented traditional segmentation techniques considering the

ISIC-2017 challenge dataset. Figure 5 demonstrates qualitative performance analysis of the proposed Active Contour Model against traditional segmentation techniques like Mask RCNN, DeepLabV3+, and Ensemble considering ISIC 2017 dataset images.
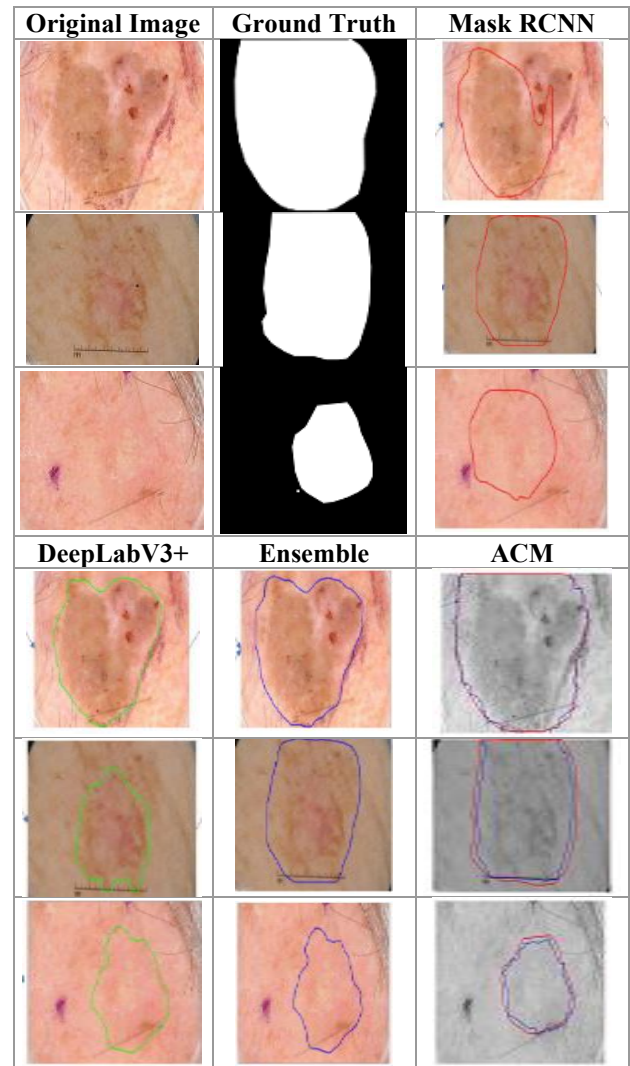

Figure 6. The results of the segmentation quality of different models with our proposed ACM

Table 4. Performance evaluation metrics (%) for lesion segmentation considering ISIC -2017 challenge dataset

Algorithm	Jaccard	Dice	Accuracy	Specificity
CDNN [31]	76.50	84.90	93.40	97.50
U-Net1[32]	76.20	84.70	93.20	97.80
U-Net2	61.60	76.30	90.10	97.20
SegNet	69.60	82.10	91.80	95.40
FrCN	77.10	87.00	94.00	96.70
Ensemble S	76.00	84.40	93.30	97.90
Ensemble L	78.80	86.60	93.90	95.50
Ensemble A	79.30	87.10	94.10	95.00
Proposed ACM	79.23	87.26	94.63	98.58

On the ISIC-2017 challenge dataset, Table 5 shows the quantitative performance comparison of the suggested ACM against a number of cutting-edge segmentation techniques. The Jaccard Index, Dice coefficient, accuracy, and specificity are among the assessed parameters. With the highest scores in the Jaccard Index (79.23), Dice coefficient (87.26), accuracy

(94.63), and specificity (98.58), ACM performs better than the other approaches, according to the data. ACM is a potential method for segmenting melanoma lesions in dermoscopic images since it shows notable improvements in segmentation accuracy and specificity.

It is evident from Figure 6 results that the segmentation quality of the ACM is quite high, and accurate edges are formed with reference to ground truth and comparison with existing techniques.

Table 5. Quantitative performance considering ISIC-2017 challenge dataset against recent state-of-art-segmentation methods

Algorithm	Jaccard	Dice	Accuracy	Specificity
FCN AlexNet	72.55	82.15	92.65	97.37
FCN-32s	72.86	82.44	92.72	96.72
FCN-16s	73.65	82.80	92.74	96.68
FCN-8s	71.87	81.06	92.52	96.87
Deeplab V3+	77.15	85.16	93.66	97.25
Mask R-CNN	77.39	85.58	93.48	96.01
Ensemble-L	78.82	86.66	93.93	95.45
Proposed ACM	79.23	87.26	94.63	98.58

4.5 Discussion

In this work, we provide an ACM for dermoscopic picture segmentation with a focus on melanoma diagnosis. In order to overcome the difficulties involved in automated dermoscopy picture recognition, the ACM was created. When compared to cutting-edge methods, the suggested ACM showed remarkable segmentation performance after rigorous testing on the PH2 and ISIC-2017 datasets.

Measurement and Evaluation

Our quantitative analysis, which is shown in Tables 1-5, emphasizes how much better the ACM is. Notably, on the PH2 dataset and the ISIC-2017 dataset, the ACM obtained segmentation accuracy of 96.77% and 94.63%, respectively. In particular, the Jaccard index, Dice coefficient, specificity, and sensitivity metrics were always much better than a range of conventional methods for segmentation. The results represent how good a job ACM does in expressing the edges of the lesions.

Superior Execution

Figures 3-6 present more qualitative analyses, further giving evidence of ACM powers. That is, the visual depictions for the ACM's ability to generate correct contours and crisp edges as opposed to other segmentation algorithms fulfill a critical need for lesion segmentation.

Experimental Configuration and Sturdiness

The experimental setup confirmed the suggested ACM's resilience by being run on a 64-bit Intel processor running Windows 10 with 16GB RAM. Such assessment metrics as segmentation accuracy, the Jaccard index, and the dice coefficient were used to gauge the performance of the model. The ACM routinely turns out performances better than other competing algorithms, thus asserting its superiority on a variety of datasets.

5. CONCLUSIONS

This paper finally introduces a precise and efficient comprehensive lesion segmentation algorithm based on ACM in lesion segmentation for melanoma detection. In this comprehensive mathematical modeling, gradient potentials, pairwise potentials, and unary potentials are included besides energy minimization solutions to enhance the accuracy of the segmentation procedure. Additionally, artifacts are removed by the use of filters and a model of the Gaussian distribution, which helps in effective contour features. Detection of edges of lesions correctly enhances segmentation efficiency.

All this can be proven by the performance evaluation that the above-mentioned ACM has done in the different datasets such as the PH2 and ISIC 2017 challenge datasets. Particularly, the ACM performs quite well on the PH2 dataset as the segmentation accuracy is high, standing at 96.77%; Jaccard index comes at 88.95%; Dice coefficient at 93.97%; specificity at 97.59%; and at 98.98%, sensitivity in the proposed ACM for the said dataset. Experimental results of different authors allow us to evaluate our model on the ISIC 2017 challenge data set. Among them, the segmentation accuracy of our developed ACM is very good, at 94.63%. The Jaccard index is 0.7923, and the Dice coefficient is 0.8726, with very good specificity.

These performance indicators underline the therapeutic significance of the proposed ACM for the enhancement of accuracy and reliability in melanoma detection, besides underlining its excellence in technology. With the advanced mathematical model and the artifact removal procedures in combination with excellent performance metrics, the ACM becomes a truly significant contribution to the field of automated diagnosis methods for skin cancers.

6. FUTURE SCOPE

Our research will investigate new approaches that could improve the prediction performance of melanoma detection. The major directions in which our future work is guided are as follows:

Integration of Hybrid methodology: We intend to present a hybrid methodology that effectively combines transfer learning, deep learning, and machine learning methods [35]. By combining the advantages of both paradigms, this integrative approach aims to produce a prediction model that is more reliable and accurate. It is expected that this all-encompassing strategy will improve melanoma detection overall.

Data Augmentation Techniques: We intend to include a variety of data augmentation techniques [36] in our methodology in order to further enhance prediction performance. We'll strategically use augmentation techniques, including rotation, flipping, and scaling. This augmentation attempts to improve the model's capacity to generalize across a range of dermatoscopic pictures in addition to addressing particular issues within the dataset.

Examination of Learning Environments: We plan to do extensive testing in a range of learning environments in the future, with a focus on active learning and transfer learning [37]. The purpose of these settings is to investigate scenarios of adaptive learning that can improve the model's ability to learn from fresh data continually and efficiently transfer information between domains.

Through the explicit mention of the use of particular data augmentation approaches and the expression of our willingness to modify our intentions going forward in light of new information, we hope to add a nuanced grasp of the dynamic character of the subject to our research agenda. This

strategy guarantees a thorough investigation of all possible directions to improve the precision and usefulness of melanoma detection techniques.

REFERENCES

[1] Celebi, M.E., Iyatomi, H., Schaefer, G., Stoecker, W.V. (2009). Lesion border detection in dermoscopy images. Computerized Medical Imaging and Graphics, 33(2): 148-153. https://doi.org/10.1016/j.compmedimag.2008.11.002

[2] Conforti, C., Giuffrida, R., Vezzoni, R., Resende, F.S., di Meo, N., Zalaudek, I. (2020). Dermoscopy and the experienced clinicians. International Journal of Dermatology, 59(1): 16-22. https://doi.org/10.1111/ijd.14512

[3] Yélamos, O., Braun, R.P., Liopyris, K., Wolner, Z.J., Kerl, K., Gerami, P., Marghoob, A.A. (2019). Dermoscopy and dermatopathology correlates of cutaneous neoplasms. Journal of the American Academy of Dermatology, 80(2): 341-363. https://doi.org/10.1016/j.jaad.2018.07.073

[4] Lucas, R.M., Yazar, S., Young, A.R., Norval, M., De Gruijl, F.R., Takizawa, Y., Rhodes, L.E., Sinclair, C.A., Neale, R.E. (2019). Human health in relation to exposure to solar ultraviolet radiation under changing stratospheric ozone and climate. Photochemical & Photobiological Sciences, 18(3): 641-680. https://doi.org/10.1039/c8pp90060d

[5] López-Leyva, J.A., Guerra-Rosas, E., Álvarez-Borrego, J. (2021). Multi-class diagnosis of skin lesions using the Fourier spectral information of images on additive color model by artificial neural network. IEEE Access, 9: 35207-35216. https://doi.org/10.1109/ACCESS.2021.3061873

[6] Bian, J., Zhang, S., Wang, S., Zhang, J., Guo, J. (2021). Skin lesion classification by multi-view filtered transfer learning. IEEE Access, 9: 66052-66061. https://doi.org/10.1109/ACCESS.2021.3076533

[7] Khan, M.A., Muhammad, K., Sharif, M., Akram, T., de Albuquerque, V.H.C. (2021). Multi-class skin lesion detection and classification via teledermatology. IEEE Journal of Biomedical and Health Informatics, 25(12): 4267-4275. https://doi.org/10.1109/JBHI.2021.3067789

[8] Ain, Q.U., Al-Sahaf, H., Xue, B., Zhang, M. (2020). Generating knowledge-guided discriminative features using genetic programming for melanoma detection. IEEE Transactions on Emerging Topics in Computational Intelligence, 5(4): 554-569. https://doi.org/10.1109/TETCI.2020.2983426

[9] National Cancer Institute. National Cancer Institute, PDQ Melanoma Treatment. Bethesda. PDQ adult treatment editorial board. https://www.cancer.gov/types/skin/hp/melanoma-treatment-pdq/, accessed on Dec. 9, 2019.

[10] Cancer Statistics Center. American Cancer Society. https://cancerstatisticscenter.cancer.org.

[11] Mathur, P., Sathishkumar, K., Chaturvedi, M., Das, P., Sudarshan, K.L., Santhappan, S., Nallasamy, V., John, A., Narasimhan, S., Roselind, F.S., Icmr-Ncdir-Ncrp Investigator Group. (2020). Cancer statistics, 2020: Report from national cancer registry programme, India. JCO Global Oncology, 6: 1063-1075. https://doi.org/10.1200/GO.20.00122

[12] Leiter, U., Keim, U., Garbe, C. (2020). Epidemiology of skin cancer: Update 2019. Sunlight, Vitamin D and Skin Cancer, 123-139. https://doi.org/10.1007/978-3-030-46227-7_6

[13] Mendonça, T., Ferreira, P.M., Marques, J.S., Marcal, A.R., Rozeira, J. (2013). PH 2-A dermoscopic image database for research and benchmarking. In 2013 35th Annual International Conference of the IEEE Engineering in Medicine and Biology Society (EMBC), pp. 5437-5440. https://doi.org/10.1109/EMBC.2013.6610779. PMID: 24110966

[14] Rehman, M., Ali, M., Obayya, M., Asghar, J., Hussain, L., Nour, M.K., Negm, N., Hilal, A.M. (2022). Machine learning based skin lesion segmentation method with novel borders and hair removal techniques. Plos one, 17(11): e0275781. https://doi.org/10.1371/journal.pone.0275781

[15] Seeja, R.D., Suresh, A. (2019). Deep learning based skin lesion segmentation and classification of melanoma using support vector machine (SVM). Asian Pacific Journal of Cancer Prevention: APJCP, 20(5): 1555. https://doi.org/10.31557/APJCP.2019.20.5.1555

[16] Xie, Y., Zhang, J., Xia, Y., Shen, C. (2020). A mutual bootstrapping model for automated skin lesion segmentation and classification. IEEE Transactions on Medical Imaging, 39(7): 2482-2493. https://doi.org/10.1109/TMI.2020.2972964

[17] Berkay, M., Mergen, E.H., Binici, R.C., Bayhan, Y., Gungor, A., Okur, E., Unay, D., Turkan, M. (2019). Deep learning based melanoma detection from dermoscopic images. In 2019 Scientific Meeting on Electrical-Electronics & Biomedical Engineering and Computer Science (EBBT), pp. 1-4. https://doi.org/10.1109/EBBT.2019.8741934

[18] Putra, T.A., Rufaida, S.I., Leu, J.S. (2020). Enhanced skin condition prediction through machine learning using dynamic training and testing augmentation. IEEE Access, 8: 40536-40546. https://doi.org/10.1109/ACCESS.2020.2976045

[19] Zhao, C., Shuai, R., Ma, L., Liu, W., Hu, D., Wu, M. (2021). Dermoscopy image classification based on StyleGAN and DenseNet201. IEEE Access, 9: 8659-8679. https://doi.org/10.1109/ACCESS.2021.3049600

[20] Pacheco, A.G., Krohling, R.A. (2021). An attention-based mechanism to combine images and metadata in deep learning models applied to skin cancer classification. IEEE Journal of Biomedical and Health Informatics, 25(9): 3554-3563. https://doi.org/10.1109/JBHI.2021.3062002.

[21] Rastghalam, R., Danyali, H., Helfroush, M.S., Celebi, M.E., Mokhtari, M. (2021). Skin melanoma detection in microscopic images using HMM-based asymmetric analysis and expectation maximization. IEEE Journal of Biomedical and Health Informatics, 25(9): 3486-3497. https://doi.org/10.1109/JBHI.2021.3081185

[22] Khetani, V., Gandhi, Y., Bhattacharya, S., Ajani, S.N., Limkar, S. (2023). Cross-domain analysis of ML and DL: Evaluating their impact in diverse domains. International Journal of Intelligent Systems and Applications in Engineering, 11(7s): 253-262.

[23] Patil, R., Bellary, S. (2021). Ensemble learning for detection of types of melanoma. In 2021 International Conference on Computing, Communication and Green Engineering (CCGE), pp. 1-6. https://doi.org/10.1109/CCGE50943.2021.9776373

[24] Razzak, I., Naz, S. (2020). Unit-vise: Deep shallow unit-vise residual neural networks with transition layer for expert level skin cancer classification. IEEE/ACM Transactions on Computational Biology and Bioinformatics, 19(2): 1225-1234. https://doi.org/10.1109/TCBB.2020.3039358

[25] Adegun, A., Viriri, S. (2021). Deep learning techniques for skin lesion analysis and melanoma cancer detection: A survey of state-of-the-art. Artificial Intelligence Review, 54(2): 811-841. https://doi.org/10.1007/s10462-020-09865-y

[26] Patil, R., Bellary, S. (2021). Transfer learning based system for melanoma type detection. Revue d'Intelligence Artificielle, 35(2): 123-130. https://doi.org/10.18280/ria.350203

[27] Kaymak, Ç., Uçar, A. (2019). Semantic image segmentation for autonomous driving using fully convolutional networks. In 2019 International Artificial Intelligence and Data Processing Symposium (IDAP), Malatya, Turkey, pp. 1-8. https://doi.org/10.1109/IDAP.2019.8875923

[28] Codella, N.C., Gutman, D., Celebi, M.E., Helba, B., Marchetti, M.A., Dusza, S.W., Kalloo, A., Liopyris, K., Mishra, N., Kittler, H., Halpern, A. (2018). Skin lesion analysis toward melanoma detection: A challenge at the 2017 international symposium on biomedical imaging (ISBI), hosted by the international skin imaging collaboration (ISIC). In 2018 IEEE 15th International Symposium on Biomedical Imaging (ISBI 2018), pp. 168-172. https://doi.org/10.1109/ISBI.2018.8363547

[29] Bi, L., Kim, J., Ahn, E., Kumar, A., Fulham, M., Feng, D. (2017). Dermoscopic image segmentation via multistage fully convolutional networks. IEEE Transactions on Biomedical Engineering, 64(9): 2065-2074. https://doi.org/10.1109/TBME.2017.2712771

[30] Chen, L.C., Papandreou, G., Kokkinos, I., Murphy, K., Yuille, A. L. (2017). Deeplab: Semantic image segmentation with deep convolutional nets, atrous convolution, and fully connected crfs. IEEE Transactions on Pattern Analysis and Machine Intelligence, 40(4): 834-848. https://doi.org/10.1109/TPAMI.2017.2699184

[31] Yuan, Y. (2017). Automatic skin lesion segmentation with fully convolutional-deconvolutional networks. arXiv preprint arXiv:1703.05165. https://arxiv.org/pdf/1703.05165.

[32] Goyal, M., Oakley, A., Bansal, P., Dancey, D., Yap, M.H. (2019). Skin lesion segmentation in dermoscopic images with ensemble deep learning methods. Ieee Access, 8: 4171-4181. https://doi.org/10.1109/ACCESS.2019.2960504

[33] Badrinarayanan, V., Kendall, A., Cipolla, R. (2017). Segnet: A deep convolutional encoder-decoder architecture for image segmentation. IEEE Transactions on Pattern Analysis and Machine Intelligence, 39(12): 2481-2495. https://doi.org/10.1109/TPAMI.2016.2644615

[34] Agrawal, G., Jha, U., Bidwe, R. (2023). Automatic facial expression recognition using advanced transfer learning. In Proceedings of the 2023 Fifteenth International Conference on Contemporary Computing, pp. 450-458. https://doi.org/10.1145/3607947.3608047

[35] Vasant Bidwe, R., Mishra, S., Kamini Bajaj, S., Kotecha, K. (2024). Attention-focused eye gaze analysis to predict autistic traits using transfer learning. International Journal of Computational Intelligence Systems, 17(1): 120. https://doi.org/10.1007/s44196-024-00491-y

[36] Bidwe, R.V., Mishra, S., Patil, S., Shaw, K., Vora, D.R., Kotecha, K., Zope, B. (2022). Deep learning approaches for video compression: A bibliometric analysis. Big Data and Cognitive Computing, 6(2): 44.

[37] Bidwe, R.V., Mishra, S., Bajaj, S. (2023). Performance evaluation of Transfer Learning models for ASD prediction using non-clinical analysis. In Proceedings of the 2023 Fifteenth International Conference on Contemporary Computing, pp. 474-483. https://doi.org/10.1145/3607947.3608050